Research Square

Preprints are preliminary reports that have not undergone peer review.
They should not be considered conclusive, used to inform clinical practice,
or referenced by the media as validated information.

Characteristics of hydrogen Lyman lines during solar cycles 23–24 and solar flares

Ryosuke Okubo

ed25007@nda.ac.jp

National Defense Academy of Japan

Kyoko Watanabe

National Defense Academy of Japan

Shinnosuke Kitajima

National Defense Academy of Japan

Satoshi Masuda

Institute for Space-Earth Environmental Research

Research Article

Keywords: Lyman series, Lymanα/β ratio, Solar Flare, Solar Cycle 23–24

Posted Date: November 4th, 2026

DOI: https://doi.org/10.21203/rs.3.rs-11371766/v1

License: This work is licensed under a Creative Commons Attribution 4.0 International License.
Read Full License

Additional Declarations: No competing interests reported.

Characteristics of hydrogen Lyman lines during solar cycles 23–24 and solar flares

Ryosuke Okubo[1], Kyoko Watanabe[1], Shinnosuke Kitajima[1], Satoshi Masuda[2]
1 National Defense Academy of Japan, 2 ISEE/Nagoya University

Abstract

Solar Extreme Ultraviolet (EUV; 10-124 nm) emissions impact the Earth's ionosphere. The Lyman-alpha line (Ly α; 121.6 nm) ionizes NO molecules in the D-region (60-100 km), while the Lyman-beta line (Ly β; 102.6 nm) ionizes O_2 in the E-region (100-150 km). Despite Ly β's weaker irradiance, the higher O_2 density in the E-region suggests Ly β could significantly influence the ionosphere. Limited Ly β observations require estimation and substitution from Ly α. Lemaire et al. (2012) analyzed the relationship between Ly α and Ly β during solar cycle 23 through fluctuations in the Ly α/β ratio and found that the Ly α/β ratio was small during solar maximum and large during solar minimum. Based on these results, we used data from the Thermosphere, Ionosphere, Mesosphere, Energetics and Dynamics (TIMED)/Solar Extreme Ultraviolet Experiment (SEE), the Solar Dynamics Observatory (SDO)/Extreme Ultraviolet Variability Experiment (EVE), and the Geostationary Operational Environmental Satellite (GOES)/Extreme Ultraviolet Sensor (EUVS)-E to derive the Ly α/β ratio during solar cycle 24 and for M-class or larger solar flares occurring between 2010 and 2014. We derived an updated third-order polynomial fit incorporating the revised instrumental calibrations reported by Lemaire et al. (2012). The long-term variation in the Ly α/β ratio during solar cycle 24 did not differ significantly from that observed during solar cycle 23. However, during flares, the Ly α/β ratio fluctuated much more rapidly than during the solar cycle. This was due to Ly β increase exceeding that of Ly α, reflecting complex nonthermal behaviors in the flaring solar atmosphere. Particularly, the strong non-LTE radiative transfer effects caused by the difference in optical thickness between the Ly α and Ly β may contribute this Ly α/β ratio decrease.

Key words

Lyman series, Lyman α/β ratio, Solar Flare, Solar Cycle 23-24

1. Introduction

Solar Hydrogen Lyman lines possess significantly strong irradiance in extreme ultraviolet (EUV; 10–124 nm) light and are expected to influence space weather.

Among EUV emissions, solar hydrogen Lyman-alpha (Ly α; 121.6 nm) has the strongest irradiance and has been extensively studied to understand its impact on the Earth's upper atmosphere. It is widely recognized that Ly α is crucial for forming and maintaining the D-region of the ionosphere (Greatorex et al., 2023; Kitajima et al., 2025). Furthermore, its impact during solar flares is thought to extend to the E-region; for instance, Milligan et al. (2020) suggested that Ly α may contribute significantly to ionization in Earth's ionospheric E-region, as inferred from the response of the Kakioka magnetometer. Such discussions illustrate that Ly α is highly regarded and continually draws attention in space weather research.

On the other hand, the next strongest hydrogen line after Ly α is the Lyman-beta line (Ly β;102.6 nm), but its irradiance is generally only about one-fiftieth to one-seventieth that of Ly α during both background solar activity and solar flare. As a result, Ly β is currently observed less frequently than Ly α, in particular, continuous high-cadence observations of Ly β suitable for flare analysis have been severely limited since 2014, and research on the short-term variation of Ly β has not progressed as much. As for the effects of these Lyman lines on the Earth's ionosphere, Ly α and Ly β have different characteristics and ionize different molecules in the Earth's atmosphere. The photon energy of Ly α is 10.20 eV, whereas that of Ly β is 12.09 eV. Theoretically, Ly α can ionize nitrogen monoxide (NO) molecules (ionization energy 9.27 eV; Dressler and Miescher, 1965), which are abundant at an altitude of approximately 70 km, while Ly β can ionize molecular oxygen (O_2) (12.07 eV ionization energy; Samson and Gardner, 1975) at an altitude of 110 km. According to Bouziane et al. (2022), the density of O_2 molecules is more than thousand times that of NO. This suggests that, despite its lower irradiance, Ly β has a sufficiently large target for ionization to warrant investigation alongside Ly α in space weather research. Given the limited availability of Ly β observations, we aim to derive a relationship between Ly α and Ly β that enables us to estimate and reconstruct Ly β from the more frequently observed Ly α. Lemaire et al. (2012) has already derived the relationship between Ly α and Ly β as the periodic variation of the Ly α/β ratio (Ly α irradiance over Ly β irradiance) from 2002 to 2010, covering the latter half of solar cycle 23 and the beginning of solar cycle 24. Ly α/β ratio is larger (around 70) in solar minimum, and smaller (around 55) in solar maximum. However, Lemaire et al. (2012) did not explain why the Ly α/β ratio exhibits such periodic variation during the solar cycle. Moreover, there have been no discussions regarding the Ly α/β ratio during solar cycle 24 or during solar flares. Thus, we included these discussions and

reported the results of the Lyman line emissions using methods similar to those of Lemaire et al. (2012).

2. Methods

To obtain the Lyman line data during solar cycles, we used the Thermosphere Ionosphere Mesosphere Energetics and Dynamics (TIMED) / EUV Grating Spectrograph-Solar EUV Experiment (EGS-SEE), which is the same instrument used by Lemaire et al. (2012). We used the TIMED SEE EGS Level 2 Data Products, version 12, released on October 31, 2017. The data cadence was one day, excluding solar flare events. The spectral resolution is 0.1 nm. In this study, the Ly α and Ly β irradiances are measured over spectral intervals of 1.0 nm (121.0 nm-122.0 nm) and 0.7 nm (102.2 nm-102.9 nm), respectively, following Lemaire et al. (2012).

For the data of Lyman lines during solar flares, we used Geostationary Operational Environmental Satellite (GOES) / Extreme Ultraviolet Sensor (EUVS)-E channel for Ly α, and Solar Dynamics Observatory (SDO) / EUV Variability Experiment (EVE), (Woods et al., 2012) for Ly β. GOES/EUVS-E observes the Ly α band with a time resolution of 1 min. GOES/EUVS data were calibrated by referencing TIMED/SEE, solar radiation and climate experiment/solar stellar irradiance comparison experiments, or SORCE/SOLSTICE (Evans et al., 2010). We used GOES-15/EUVS-E version 4, released on September 14, 2016. The SDO/EVE provides a time resolution of 10 s and a spectral resolution of 0.02 nm. We also apply a 0.7 nm interval for Ly β to ensure comparability between the flare data and the solar cycle data. The EVE had two channels: multiple EUV grating spectrographs (MEGS)-A and MEGS-B. MEGS-A covers wavelengths ranging from 6 to 37 nm, whereas MEGS-B covers wavelengths ranging from 37 to 106 nm. In this study, the MEGS-B channel was used. The dataset used was EVE/L2, version 7, which was released on June 29, 2021.

To compare the temporal variations of the Lyman lines with soft X-rays, we used the GOES/X-Ray Sensor (XRS); specifically, we used the B-channel, which ranged from 1 to 8 Å. This band is the standard for determining the solar flare classes. Corrected flux values were applied based on the GOES/XRS data quality report by Machol and Codrescu (2024). Specifically, we multiplied the flux by factors ranging from 100/141 to 100/148, depending on the soft X-ray flux during flare events.

3. Results

3.1. Lyman lines during solar cycle variation

In this section, we report the results of the Ly α / β ratio from 2002 to 2016 (solar cycles 23 and 24) using the method of Lemaire et al. (2012). Figure 1 shows the long-term variations in the Lyman lines over this period, revealing no significant difference

between the variation patterns of Ly α and Ly β. However, when examining the relative irradiance increase from minimum to maximum values, the ratio of Ly α is 1.90, while that of Ly β is 2.60. This indicates that Ly β varies more than Ly α during solar cycles.

Figure 2 presents the Ly α/β ratio in the same period as Figure 1. The blue dots represent solar cycle 23 (from February 2002 to mid-December 2008), and the red dots represent solar cycle 24 (from the end of 2008 to January 2016). The blue and red solid lines represent the linear fits of the blue and red dots, respectively, derived using the least-squares method. The gray-hatched area represents the propagated error from the measurement uncertainties of Ly α and Ly β. We also plot both the third-order polynomial fit derived by Lemaire et al. (2012) and the updated third-order polynomial fit derived in this study.

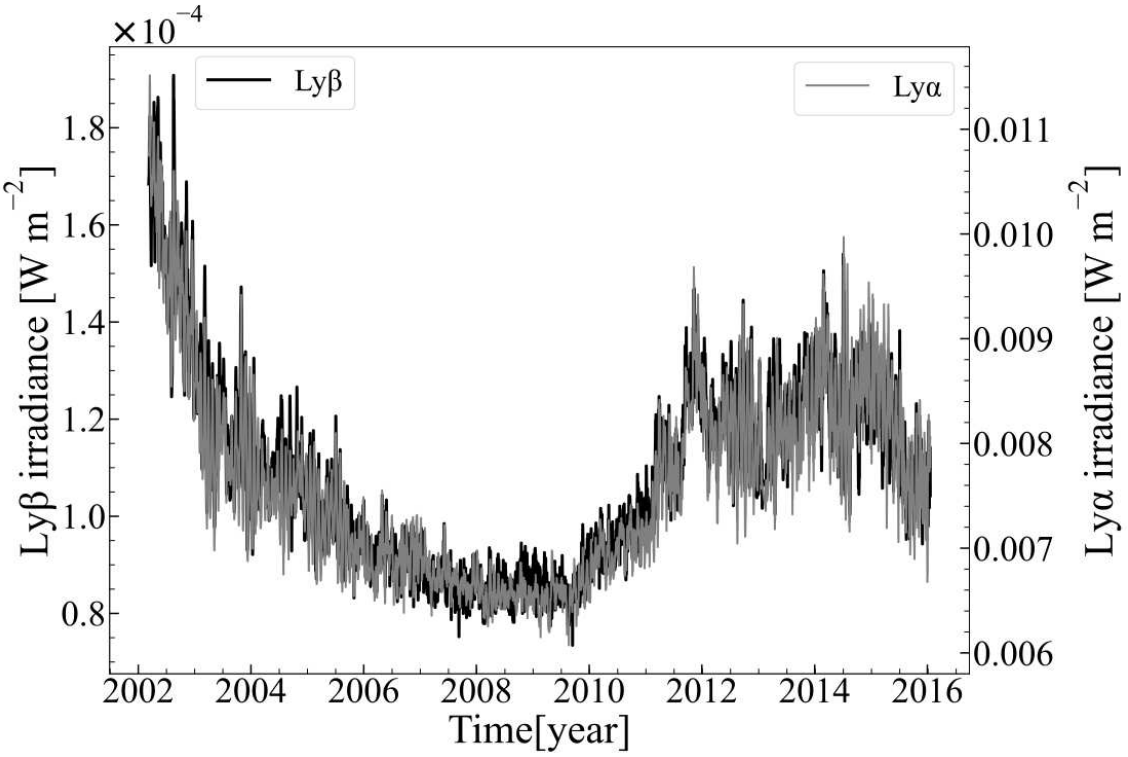


Figure1 Long time variation of Ly α (gray) and Ly β (black) from 2002 to 2010 by TIMED/EGS-SEE. Ly α (right axis) and Ly β (left axis) are scaled by their maximum and minimum value.

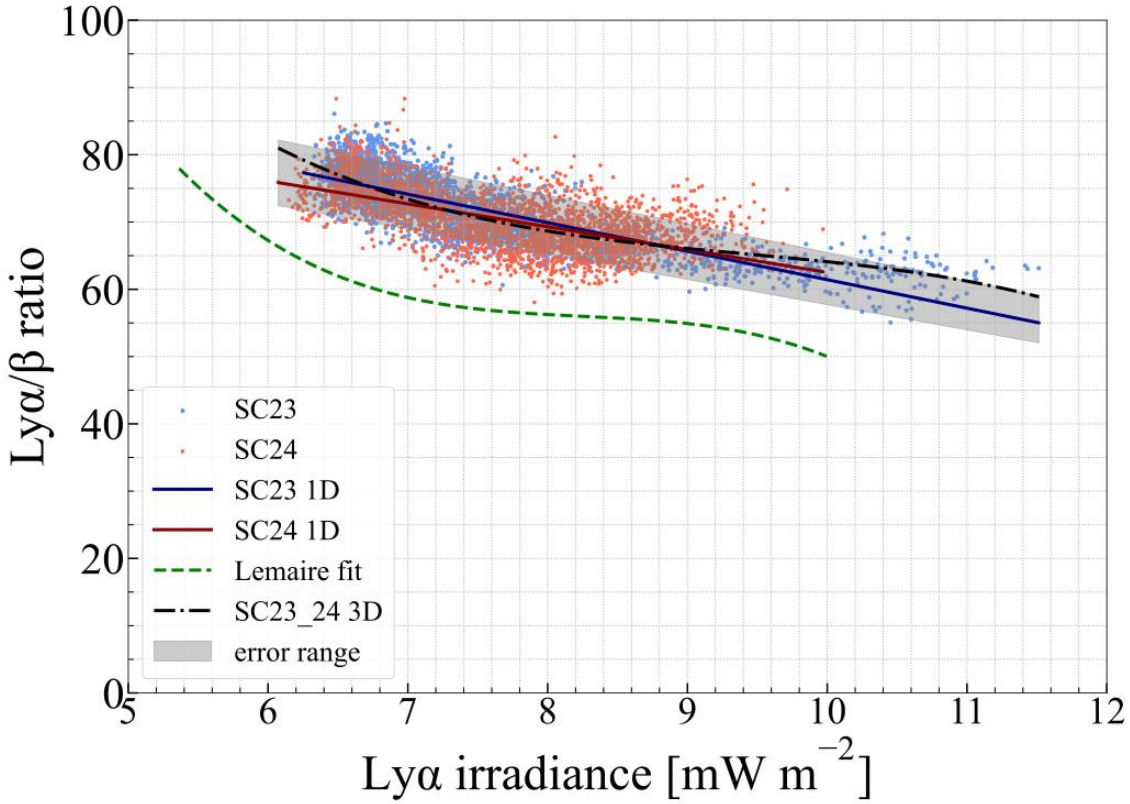


Figure 2 Ly α/β ratio as a function of Ly α irradiance from 2002 to 2016. Plot with the y-axis range set to 0–100, matching the scale of Lemaire et al. (2012). blue dots and the solid blue line represent solar cycle 23 (2002–2008) and its linear fit, respectively. Red dots and the solid red line represent solar cycle 24 (2008–2016) and its linear fit. The green dashed line indicates the third-order polynomial fit derived by Lemaire et al. (2012). The black dash-dot line shows the updated third-order polynomial fit for the combined dataset of solar cycles 23 and 24. The gray-shaded area represents the error range of the Ly α/β ratio. SC: solar cycle.

The linear fits of Ly α irradiances and Ly α/β ratio during solar cycle 23 and 24 in Figure 2 are represented by Equations (1) and (2) below:

$$I_{\alpha 23}/I_{\beta 23} = -4.2 \times 10^3 I_{\alpha 23} + 104 \quad (1)$$

$$I_{\alpha 24}/I_{\beta 24} = -3.4 \times 10^3 I_{\alpha 24} + 97 \quad (2)$$

Here, $I_\alpha (I_\beta)$ denotes Ly α (Ly β) irradiance, and I_α/I_β represents Ly α/β ratio. The subscripts "α" and "β" correspond to Ly α and Ly β, respectively. Similarly, "23,"

"24," and "23_24" denote solar cycles 23, 24, and combined period of 23 and 24, respectively. For example, $I_{\alpha 23}$ refers to the Ly α irradiance during solar cycle 23. Furthermore, a linear fit over the full interval spanning solar cycles 23 and 24 yields Equation (3):

$$I_{\alpha 23_24}/I_{\beta 23_24} = -4.0 \times 10^3 I_{\alpha 23_24} + 101 \quad (3)$$

Solar cycle 23 is more active than cycle 24, as evident from Figure 1, resulting in a larger variation in the Ly α/β ratio during solar cycle 23 in Figure 2.

Figure 2 , Equation (1) and (2) suggests a downward slope in the relationship between Ly α and Ly α/β ratio during solar cycle 23 and 24, indicating a negative coefficient for I_α. This overall downward trend is consistent with the findings of Lemaire et al. (2012). For further comparison with our results, we overlaid the third-order polynomial fit reported by Lemaire et al. (2012) as a green dashed line in Figure 2. They expressed the Ly α/β ratio as a function of Ly α irradiance (in mWm^{-2})
Using the following Equation (4):

$$R_{Lemaire} = 511.0 - 163.5 I_{Ly\alpha} + 19.70 I_{Ly\alpha}^2 - 0.796 I_{Ly\alpha}^3 \quad (4)$$

As shown in Figure 2, the curve from Lemaire et al. (2012) is systematically shifted toward the lower left compared with our data distribution. This discrepancy can be attributed to differences in the calibration versions of the TIMED/SEE Level 2 datasets. Lemaire et al. (2012) utilized an older data version, in which the absolute Ly α irradiance was calibrated to a lower range (approximately 5–10 mWm^{-2}). In contrast, our study used the updated version 12 dataset released in 2017. According to the official TIMED/SEE Level 2 data product documentation (README file), this newer version incorporates continuous corrections for instrument degradation trends and was validated against SDO/EVE calibration flights up to 2016. Additionally, official time-series data provided by the Laboratory for Atmospheric and Space Physics (LASP) confirm that the Version 12 Ly α irradiance typically fluctuates between 6 and 11 mWm^{-2}, aligning with the data distribution observed in our study (https://lasp.colorado.edu/see/data/daily-averages/level-2-egs/egs-time-series/).

Therefore, by utilizing the combined dataset of solar cycles 23 and 24 based on the latest calibration, we derived an updated third-order polynomial fit (shown by the

black dashed–dotted line in Figure 2). The updated equation (Equation 5) is expressed as follows:

$$R_{3D} = c_0 + c_1 I_{Ly\alpha} + c_2 I_{Ly\alpha}^2 + c_3 I_{Ly\alpha}^3 \quad (5)$$

where the coefficients, along with their 1σ standard errors, are calculated as $c_0 = 293.85\ (\pm 17.59)$, $c_1 = -69.10\ (\pm 6.45)$, $c_2 = 7.1457\ (\pm 0.7793)$, and $c_3 = -0.25329\ (\pm 0.03100)$. This newly derived fit represents a more accurate physical state based on the current standard calibration.

Next, we estimate the errors of Ly α/β ratio through the error propagation from Ly α and Ly β. The result shows that the Ly α/β ratio error ranges from ± 3.50 to 4.87, with $I_{\alpha 23_24}/I_{\beta 23_24}$ of Equation (3) as a true value. As shown in Figure 2, the two lines expressed by Equations (1) and (2) fall within the error range, indicating no significant difference between Equations (1) and (2).

3.2. Lyman lines during solar flares

First, we selected the flare events that were analyzed in this study. We use the data of GOES/EUVS-E for Ly α and SDO-EVE (MEGS-B) for Ly β. The period during which both instruments were simultaneously observed was from May 1, 2010, to May 26, 2014. During this period, the SDO/EVE flare list recorded 92 flares of class M or larger. We select events that showed a clear increase (> 1 %) in Ly α irradiance, defined as instances where the irradiance at the flare end remained higher than at the flare start. As a result, 40 events were selected, including 5 X-class flares and 35 M-class flares. Table 1 lists the times, classes, and locations of the 40 solar flares selected for this study. The correlation between the Ly α/β ratio and Ly α irradiance, as well as the slope of the linear fitting, are presented in the rightmost columns of Table 1.

Table 1 Flare events in this study with correlation coefficients between Ly α irradiance and Ly α/β ratio and slopes of fitting line

No.	Time of flare-start (UT)	Class	Location of Flare	Correlation coefficient	Slope of Fitting line
1	2011 Feb. 14 17:20	M2.2	S20W04	−0.98	-1.0×10^4
2	2011 Feb. 15 01:44	X2.2	S20W10	−0.98	-1.6×10^4
3	2011 Feb. 16 01:32	M1.0	S20W42	−0.66	-1.8×10^4

4	2011 Feb. 16 07:35	M1.1	S19W29	−0.63	-1.5×10^{4}
5	2011 Feb. 16 14:19	M1.6	S21W30	−0.93	-1.4×10^{4}
6	2011 Feb. 18 14:00	M1.0	N19W00	−0.76	-1.0×10^{4}
7	2011 Mar. 07 19:43	M3.7	N30W48	−0.80	-8.7×10^{3}
8	2011 July 30 02:04	M9.3	N12E45	−0.98	-1.4×10^{4}
9	2011 Aug. 03 04:29	M1.7	N16E10	−0.92	-1.1×10^{4}
10	2011 Aug. 04 03:41	M9.3	N16W38	−0.95	-1.0×10^{4}
11	2011 Sep. 09 12:39	M1.2	N15W50	−0.34	-4.8×10^{3}
12	2011 Sep. 25 04:31	M7.4	N08E55	−0.82	-1.4×10^{4}
13	2011 Sep. 25 02:27	M4.4	N22W87	−0.81	-1.9×10^{4}
14	2011 Nov. 03 23:28	M2.1	N20E62	−0.64	-1.7×10^{4}
15	2011 Nov. 03 20:16	X1.9	N22E16	−0.97	-1.4×10^{4}
16	2011 Nov. 05 20:31	M1.8	N21E37	−0.48	-1.0×10^{4}
17	2011 Nov. 15 22:27	M1.1	N18W81	−0.60	-8.4×10^{3}
18	2011 Dec. 26 20:12	M2.3	S21W44	−0.85	-2.7×10^{4}
19	2012 Mar. 07 00:02	X5.4	N18E31	−0.96	-1.2×10^{4}
20	2012 Mar. 07 01:05	X1.3	N15E41	−0.82	-1.0×10^{4}
21	2012 Mar. 14 15:08	M2.8	N13E05	−0.58	-3.7×10^{3}
22	2012 May 10 20:20	M1.7	N12E12	−0.94	-1.1×10^{4}
23	2012 June 30 18:26	M1.6	N14E18	−0.59	-6.6×10^{3}
24	2012 July 01 19:11	M2.8	N14E04	−0.94	-9.1×10^{3}
25	2012 July 02 19:59	M3.8	S17E00	−0.78	-5.7×10^{3}
26	2012 July 05 21:37	M1.6	S12W36	−0.95	-7.6×10^{3}
27	2012 July 06 10:24	M1.8	N16E84	−0.50	-9.1×10^{3}
28	2012 Aug. 18 03:04	M1.8	N19E86	−0.47	-1.5×10^{4}
29	2013 Arp. 12 19:52	M3.3	N21W42	−0.76	-1.9×10^{4}
30	2013 Oct. 15 23:31	M1.3	S23W20	−0.90	-8.5×10^{3}
31	2013 Oct. 26 09:17	M1.5	S50E58	−0.67	-6.9×10^{3}
32	2014 Jan. 01 18:40	M9.9	S14W47	−0.87	-6.0×10^{3}
33	2014 Jan. 04 19:05	M4.0	S11E34	−0.57	-9.1×10^{3}
34	2014 Jan. 07 18:04	X1.2	S15W11	−0.69	-4.0×10^{3}
35	2014 Jan. 31 15:32	M1.1	N07E34	−0.75	-8.2×10^{3}
36	2014 Feb. 02 16:24	M1.0	N09E06	−0.76	-9.0×10^{3}
37	2014 Feb. 02 14:01	M1.3	N12E14	−0.89	-8.7×10^{3}
38	2014 Feb. 14 16:33	M1.0	S13W32	−0.88	-1.0×10^{3}
39	2014 Mar. 10 15:21	M1.7	S17E41	−0.91	-9.2×10^{3}
40	2014 May 08 09:59	M5.2	N08E54	−0.72	-8.1×10^{3}

The time evolution of Ly α and Ly β during solar flares, as listed in Table 1, is analyzed. As a representative example, we report the X5.4-class flare event, the largest flare in our event list, that occurred on March 7, 2012. Figure 3 shows the time evolution of Ly α and Ly β for this event (Event No.19). The flare lasted for 38 min from start to end. The temporal profiles of Ly α and Ly β are nearly identical, a pattern observed across all 40 flare events.

Next, we examined the relative irradiance compared to the irradiance at flare start. The relative irradiance of Ly β is constantly higher than that of Ly α. In this event, the relative irradiance of Ly α is 1.14 (13.7% increase), while that of Ly β is 1.38 (37.9% increase). This trend is consistent across all flare events, where average relative irradiance is 1.105 (10.5% increase) for Ly β and 1.044 (4.4% increase) for Ly α.

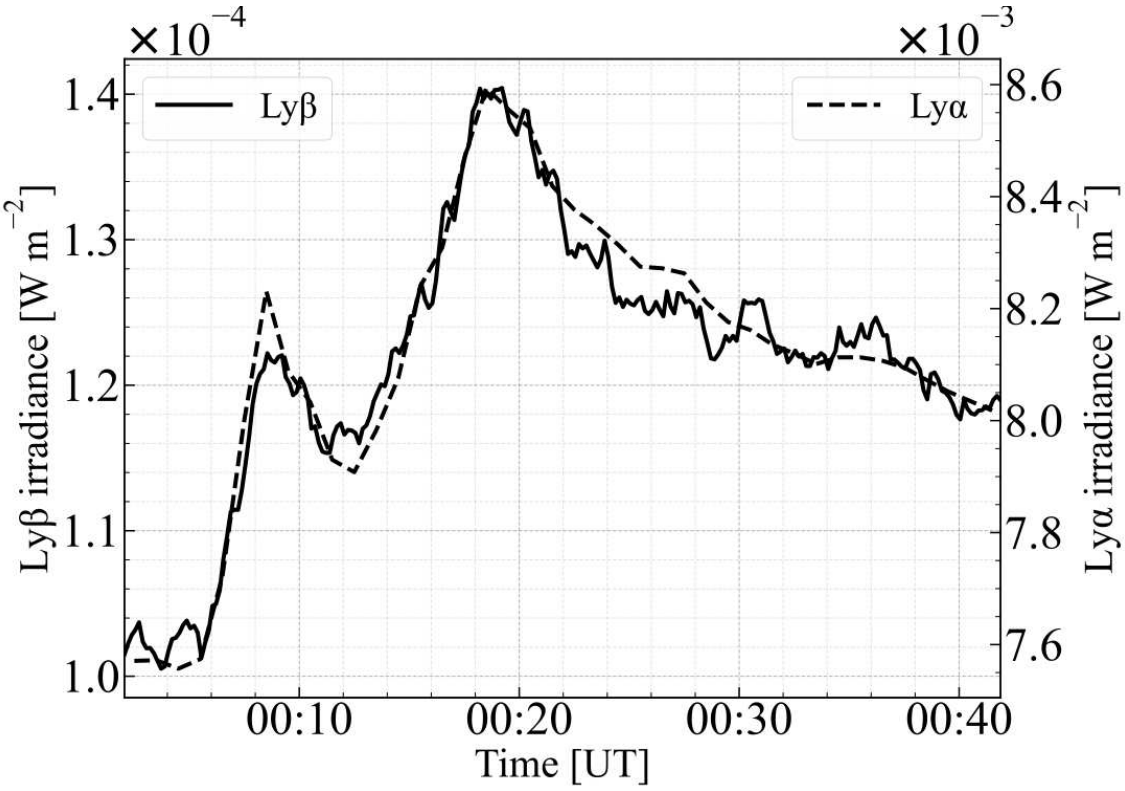


Figure 3 Time evolution of Ly α (dashed line) and Ly β (solid line) during the X5.4-class flare on 2012 March 7. Both Ly α (right axis) and Ly β (left axis) are scaled by their maximum and minimum value.

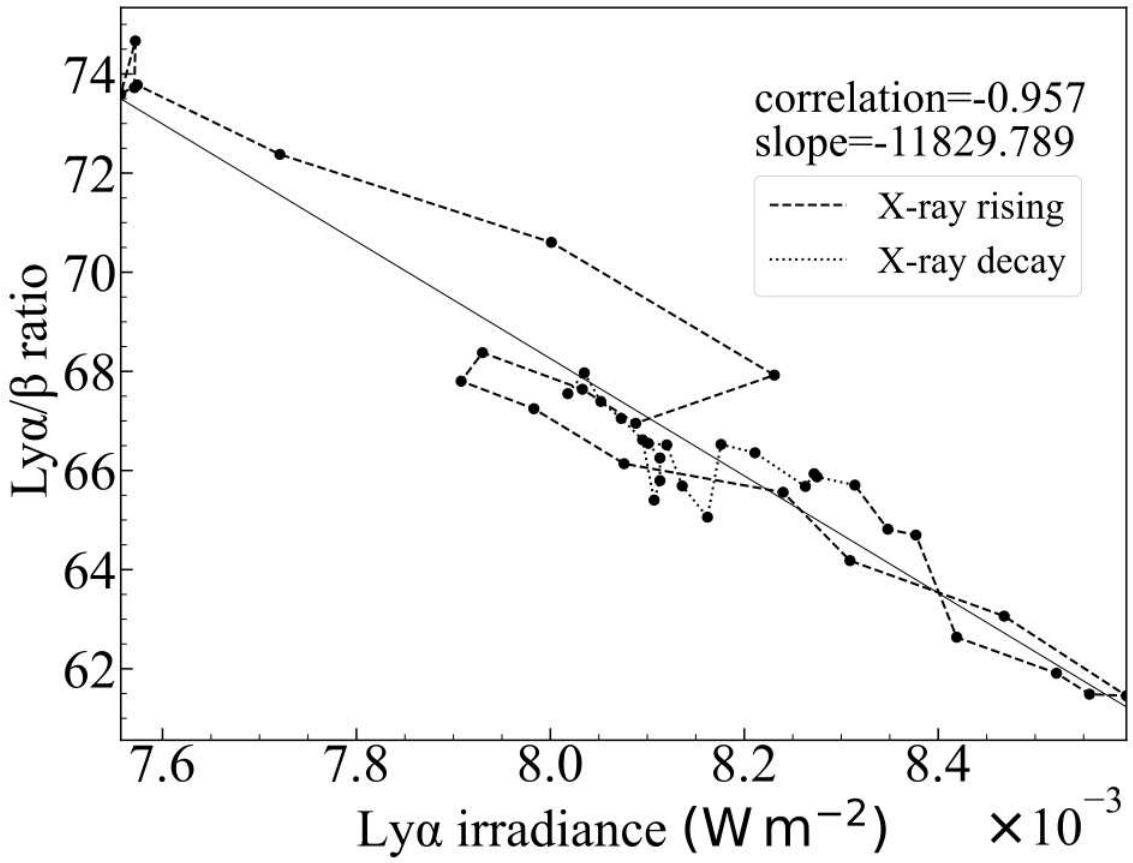


Figure 4 Ly α / β ratio as a function of Ly α irradiance for the event of Figure 3. Dashed line represents flare-start to peak, X-ray rising phase. Dotted line represents flare-peak to end, X-ray decay phase. Solid line represents linear fit.

Next, we research the relationship between the Ly α / β ratio and Ly α irradiance during solar flares. Figure 4 shows the results of the X5.4-class flare on March 7, 2012. The dashed and dotted lines represent the values during the X-ray rising and decay phases, respectively. At the flare start, the ratio is 73.5, which decreases as the Ly α irradiance increases. The correlation coefficient (CC) between Ly α irradiance and the Ly α / β ratio is −0.96, indicating a strong negative correlation close to a perfect linear downward slope (CC: −1.0). This suggests a linear relationship between Ly α irradiance and the Ly α / β ratio. The slope of the linear fitting in Figure 4 is approximately -1.2×10^4.

Table 1 shows a trend similar to that shown in Figure 4 across all 40 flare events. Out of the 40 events, 28 events exhibit a CC of less than −0.7, indicating a strong negative correlation. The correlation weakened for smaller flares, likely because of their smaller relative irradiances. The average slope of the linear fit for all 40 events is -1.0×10^4. In comparison, the slope between the Ly α / β ratio and Ly α irradiance

during solar cycles is -4.0×10^3 as seen in Equation (3). This indicates that the rate of decrease in the Ly α/β ratio during flares is approximately 2.5 times steeper than during solar cycles.

There is an X-class event, event No. 34, which occurred on January 7th, 2014 where the slope of the Ly α/β ratio versus Ly α irradiance is relatively gentle for an X-class flare. This is likely because the spatial scale of the active regions increases and is closely associated with increasing sunspot numbers, which are linked to a higher frequency of flares. Peleg et al. (2024) reported that during periods of frequent flare activity, the background X-ray flux tends to increase, particularly during long-duration events. Under such conditions, the disk-integrated Ly α/β ratio is less influenced by flare regions and more by non-flaring active regions. Therefore, we believe that the Ly α/β ratio during this period is strongly influenced by the solar maximum of solar cycle 24.

4. Discussions

When examining the relationship between Ly α and Ly β, Ly α/β ratio decreases as Ly α irradiance increases during both solar cycles and solar flares. This indicates that the relative irradiance of Ly β is greater than that of Ly α. We examine whether the relationship between Ly α and the Ly α/β ratio obtained in Section 3.1 can be explained by the FAL (Fontenla, Avrett, and Loeser) model of Fontenla et al. (1991). The FAL model was specifically designed to reproduce the EUV behavior in the chromosphere and transition region based on observations. It estimates the origin of the EUV emissions at different altitudes. Although the Ly α/β ratios from the FAL model and Equation (3) in this paper show similar trends, their slopes differ. However, they share a common qualitative characteristic: the Ly α/β ratio decreases as Ly α increases. Regarding the comparison of the results in Section 3.1. and 3.2., the slope of Ly α/β ratio as a function of Ly α is 4.0×10^3 for solar cycles, as seen in Equation (3), and 1.0×10^4 for solar flares, as discussed in Section 3.2.1. This suggests that the Ly α/β ratio varies or decreases more during solar flares than during solar cycles. This higher relative irradiance of Ly β compared to Ly α is likely due to the higher temperatures in the solar atmospheric regions where these emissions are produced. The number of particles at a given energy level can be expressed using the Boltzmann distribution, which is the ratio of the number of particles at another energy level. The hydrogen Lyman series consists of bright emission lines produced when electrons transition to the base energy level, where the principal quantum number $n = 1$. Ly α corresponds to transitions from $n = 2$, with an energy level E_2 of 10.2 eV, while Ly β corresponds to transitions from n =3, with energy level E_3 of 12.09 eV. The ratio of the upper-level populations N_3

$/N_2$, where each term corresponds to Ly β and Ly α transitions respectively, is expressed by Equation (6) in terms of their statistical weights (degeneracies), w_2 and w_3:

$$\frac{N_3}{N_2} = \frac{w_3}{w_2} e^{-\frac{E_3 - E_2}{kT}} = \frac{w_3}{w_2} e^{-\frac{h\nu}{kT}} \tag{6}$$

In Equation (6), k is the Boltzmann constant (1.38×10^{-23} J/K), T [K] is the absolute temperature, h is the Plank constant (6.63×10^{-34} J・s), and ν [Hz] is frequency. The degeneracy of the hydrogen atom was proportional to n^2, meaning w_3 / w_2 = 9/4. Thus, N_3 / N_2 varies only as a function of the temperature T; as T increases, so does the ratio N_3 / N_2. Based on this relationship, relative irradiance of Ly β increases more rapidly than that of Ly α at higher temperatures, which is qualitatively consistent with the observational trends in this study.

Next, we examine whether Equation (6) could quantitatively explain the relationship between Ly α and Ly β. However, theoretical calculations did not match the observed values. The Boltzmann distribution alone cannot quantitatively account for the electron populations that give rise to the Lyman lines, as the Ly α/β ratio deviates from the predicted value. According to Rybicki and Lightman (2004), the Boltzmann equation is valid only when the emission source is in a local thermal equilibrium (LTE). However, the Boltzmann distribution is not applicable in this case, indicating that the solar atmosphere exhibits strong non-LTE (NLTE) behavior. This implies that the local temperature alone does not determine the energy population of the particles. In the chromosphere, Lyman series emission lines are primarily formed when neutral hydrogen is collisionally excited by electrons and subsequently emits a photon upon returning to the ground state (radiative de-excitation). A crucial physical property here is that the hydrogen Lyman series is "optically thick" in the chromosphere. The emitted photons do not escape directly into space but undergo multiple absorptions and re-emissions (scattering) by surrounding hydrogen atoms.

An increase in Ly α emission during flares or solar maxima indicates an enhancement of downward heat conduction flux (or electron precipitation) from the corona. This intense heat input pushes the transition region—the boundary between the corona and the chromosphere—downward, thereby increasing the column density of the uppermost chromosphere where Lyman lines are emitted.

The core of the mechanism explaining the variation in the Ly α / β ratio lies in this increased column density combined with the difference in the optical thickness (τ) of each line. Although both Ly α and Ly β are optically thick, Ly α is inherently much thicker due to the difference in quantum mechanical oscillator strengths (the

oscillator strength of Ly α is about 5.3 times that of Ly β) (Chaffin et al., 2022). As solar activity rises and column density increases, the intensities of both lines gradually approach saturation. However, because Ly α is optically thicker, it experiences strong self-reversal effects earlier and saturates faster than Ly β. This difference in self-absorption strength has been empirically demonstrated by quiet-Sun observations, where almost all Ly α profiles exhibit strong self-reversal, while a certain fraction of the relatively optically thinner Ly β profiles do not exhibit self-reversal (Tian et al., 2009).

Consequently, as the chromospheric column density increases, the growth rate of the optically thicker Ly α intensity is strongly suppressed, whereas the Ly β intensity continues to increase relatively more, resulting in a decrease in the observed Ly α / β ratio. As shown in Section 3.2, the slope of the Ly α / β ratio during flares was about 2.5 times steeper than that during solar cycles. This can be attributed to the rapid energy release from magnetic reconnection during flares, which causes localized plasma heating and injects an even stronger heat conduction flux into the chromosphere. This causes a much more rapid increase in the column density of the emitting layer compared to non-flaring periods. The resulting strong saturation effect (intense self-absorption of Ly α) driven by the difference in optical thickness becomes remarkably prominent, leading to the observed steeper decline in the ratio.

5. Conclusion

To compare the behavior of highly irradiated Ly α with that of Ly β, which is known to influence Earth's ionosphere, we expanded upon the work of Lemaire et al. (2012) by updating the long-term irradiance relationship using newer calibration datasets from solar cycles 23 and 24, and investigated the behavior of Lyman lines during solar flares that occurred throughout Solar Cycle 24.

During solar cycles, Ly α and Ly β exhibit similar variations; however, the Ly α/ β ratio decreases as Ly α irradiance increases. During solar flares, the relative irradiance of Ly β is more than twice that of Ly α, and the slope of the relationship between the Ly α/β ratio and Ly α is 2.5 times steeper than that observed during the solar cycle.

This result likely reflects temperature differences in the formation regions where Ly α and Ly β form, suggesting that Ly β originates from a higher and hotter atmospheric layer than Ly α. Furthermore, the Ly α/β ratio deviates from the value predicted by the Boltzmann distribution, likely reflecting the influence of both temperature and nonthermal factors, including magnetic fields and nonlocal effects. This deviation is driven by the difference in optical thickness under non-LTE

conditions. As chromospheric column density increases, the intrinsically thicker Ly α experiences stronger self-absorption and saturates earlier than Ly β. The steeper gradient during flares likely results from a rapid column density increase driven by intense downward heat conduction following magnetic reconnection.

The local Ly α/β ratio during solar flares warrants further investigation. Additionally, a quantitative estimation of the contribution of nonthermal factors—such as MHD waves and magnetic fields—to the decrease in the Ly α/β ratio, combined with precise radiative transfer modeling of column density and optical depth variations, could provide deeper insights into the dynamics of this phenomenon.

Acknowledgments

This study was supported by the Collaborative Research Promotion in 2024 of the Institute for Space-Earth Environmental Research (ISEE), Nagoya University. This support provided valuable opportunities for discussion with solar physics researchers at the ISEE.

We express our gratitude to Dr. Tetsuya Watanabe of the National Astronomical Observatory of Japan for providing the opportunity to discuss and provide valuable comments on this research.

We used data from TIMED/EGS-SEE, GOES/XRS(EUVS-E), and SDO/EVE. We are grateful for access to these datasets, which enabled the data analysis and discussions conducted in this study.

Declarations

Funding

This study was supported by the Grant for Collaborative Research Promotion in 2024 from the Institute for Space-Earth Environmental Research (ISEE), Nagoya University. This research was also supported by the Japan Society for the Promotion of Science (JSPS) KAKENHI Grant Number 22K03710.

Competing Interests

The authors have no relevant financial or non-financial interests to disclose.

Author Contributions

R. O. and K. W. conceived and designed the study. S. K. provided support for the material preparation, data collection, and analysis. S. M. provided domain expertise in solar physics to interpret the results. All the authors have read and approved the final manuscript.

Data Availability

The datasets analyzed during the current study are publicly available. The TIMED/EGS-SEE data can be accessed at [https://lasp.colorado.edu/see/data/daily-averages/level-2-egs/]. The GOES15/XRS data are available at [https://www.ncei.noaa.gov/data/goes-space-environment-monitor/access/science/xrs/goes15/gxrs-l2-irrad_science/]. GOES/EUVS-E data are obtained at [https://www.ncei.noaa.gov/data/goes-space-environment-monitor/access/science/euvs/goes15/geuv-l2-avg1m/]The SDO/EVE data can be found at [https://lasp.colorado.edu/eve/data/].

Compliance with Ethical Standards

This article does not contain any studies involving human participants or animals performed by any of the authors.

References

Bouziane, A., Ferdi, M.A., Djebli, M.: 2022, Adv. Space Res. 69, 905. https://doi.org/10.1016/j.asr.2021.10.019

Chaffin, M.S., Deighan, J., Jain, S., Holsclaw, G., AlMazmi, H., Chirakkil, K., et al.: 2022, Geophys. Res. Lett. 49, e2022GL099851. https://doi.org/10.1029/2022GL099851

Dressler, K., and Miescher, E.: 1965, Astrophys. J. 141, 1266. https://doi.org/10.1086/148211

Evans, J.S., Strickland, D.J., Woo, W.K., McMullin, D.R., Plunkett, S.P., Viereck, R.A., et al.: 2010, Solar Phys. 262, 71. https://doi.org/10.1007/s11207-009-9491-x

Fontenla, J.M., Avrett, E.H., Loeser, R.: 1991, Astrophys. J. 377, 712. https://doi.org/10.1086/170399

Greatorex, H.J., Milligan, R.O., Chamberlin, P.C.: 2023, Astrophys. J. 954, 120. https://doi.org/10.48550/arXiv.2306.16234

Kitajima, S., Watanabe, K., Jin, H., Tao, C., Nishioka, M.: 2025, J. Space Weather Space Clim. 15, 10. https://doi.org/10.1051/swsc/2025008

Lemaire, P., Vial, J.-C., Curdt, W., Schühle, U., Woods, T.N.: 2012, Astron. Astrophys. 542, L25. https://doi.org/10.1051/0004-6361/201219026

Machol, J., and Codrescu, S.: 2024, Readme for GOES-R XRS L2 Data, NOAA/National Centers for Environmental Information (NCEI). https://data.ngdc.noaa.gov/platforms/solar-space-observing-satellites/goes/goes16/l2/docs/GOES-R_XRS_L2_Data_Readme.pdf

Milligan, R.O.: 2021, Solar Phys. 296, 51. https://doi.org/10.1007/s11207-021-01796-3

Milligan, R.O., Hudson, H.S., Chamberlin, P.C., Hannah, I.G., Hayes, L.A.: 2020, Space Weather 18, 7. https://doi.org/10.1029/2019SW002331

Peleg, Y., Babayew, R., Orion, I.: 2024, Int. J. Astron. Astrophys. 14, 149. https://doi.org/10.4236/ijaa.2024.143009

Rybicki, G.B., and Lightman, A.P.: 2004, Radiative Processes in Astrophysics, WILEY-VCH Verlag GmbH & Co. KGaA, 259.

Samson, J.A.R., and Gardner, J.L.: 1975, Can. J. Phys. 53, 18. https://doi.org/10.1139/p75-244

Tian, H., Curdt, W., Marsch, E., Schühle, U.: 2009, Astron. Astrophys. 504, 239. https://doi.org/10.1051/0004-6361/200811445

Woods, T.N., Eparvier, F.G., Hock, R., Jones, A.R., Woodraska, D., Judge, D., et al.: 2012, Solar Phys. 275, 115. https://doi.org/10.1007/s11207-009-9487-6

Figure Legends

Figure1 Long time variation of Ly α (gray) and Ly β (black) from 2002 to 2010 by TIMED/EGS-SEE. Ly α (right axis) and Ly β (left axis) are scaled by their maximum and minimum value.

Figure 2 Ly α / β ratio as a function of Ly α irradiance from 2002 to 2016. Plot with the y-axis range set to 0–100, matching the scale of Lemaire et al. (2012). Blue dots and the solid blue line represent solar cycle 23 (2002–2008) and its linear fit, respectively. Red dots and the solid red line represent solar cycle 24 (2008–2016) and its linear fit. The green dashed line indicates the third-order polynomial fit derived by Lemaire et al. (2012). The black dash-dot line shows the updated third-order polynomial fit for the combined dataset of solar cycles 23 and 24. The gray-shaded area represents the error range of the Ly α / β ratio. SC: solar cycle.

Figure 3 Time evolution of Ly α (dashed line) and Ly β (solid line) during the X5.4-class flare on 2012 March 7. Both Ly α (right axis) and Ly β (left axis) are scaled by their maximum and minimum value.

Figure 4 Ly α / β ratio as a function of Ly α irradiance for the event of Figure 3. Dashed line represents flare-start to peak, X-ray rising phase. Dotted line represents flare-peak to end, X-ray decay phase. Solid line represents linear fit.

Table Legend

Table 1 Flare events in this study with correlation coefficients between Ly α irradiance and Ly α / β ratio and slopes of fitting line

Acronyms and technical terms

EUV: Extreme ultraviolet, ranging from the wavelength 10 nm to 124 nm
FAL model: Fontenla, Avrett, Loeser (Fontenla et al., 1991) model
GOES/EUVS: Geostationary Operational Environmental Satellite (GOES) / Extreme Ultraviolet Sensor (EUVS)
GOES/XRS: GOES/X-Ray Sensor
LTE: Local-thermal-equilibrium
Ly α : Lyman-alpha line
Ly α/β ratio: Lyman-alpha irradiance over Lyman-beta irradiance
Ly β : Lyman-beta line
NLTE: non-local-thermal-equilibrium
Relative irradiance: the ratio of irradiance increases from minimum value
SC: Solar Cycle
SDO/EVE: Solar Dynamics Observatory (SDO)
TIMED/EGS-SEE: Thermosphere Ionosphere Mesosphere Energetics and Dynamics (TIMED) / EUV Grating Spectrograph-Solar EUV Experiment (EGS-SEE))

Symbols

c_0, c_1, c_2, c_3: Coefficients of the updated equation (Equation 5 , R_{3D})
E_2, E_3[eV]: Energy level of $n = 2$ and $n = 3$
h[6.63×10^{-34} J・s]: Plank constant
$I_{\alpha 23}, I_{\beta 23}$[W/m2]: Irradiances of Ly α and Ly β during solar cycle 23. Similarly, "23," "24," and "23_24" denote solar cycles 23, 24, and combined period of 23 and 24, respectively.
n: principal quantum number of hydrogen atom
$R_{Lemaire}$: Regression curve defined by Lemaire et al. (2012).
R_{3D}: Updated third-order polynomial fit in this study
T[K]: Absolute temperature
ν[Hz]: frequency
w_2, w_3: statistical weight or degeneracy of hydrogen atom with $n = 2$ and $n = 3$